5234 *Inorg. Chem.* **2009**, *48*, 5234–5243
DOI: 10.1021/ic900223f

Inorganic Chemistry
Article

Cobalt Complex as Building Blocks: Synthesis, Characterization, and Catalytic Applications of $\{Cd^{2+}-Co^{3+}-Cd^{2+}\}$ and $\{Hg^{2+}-Co^{3+}-Hg^{2+}\}$ Heterobimetallic Complexes

Anurag Mishra,[†] Afsar Ali,[†] Shailesh Upreti,[‡] M. Stanley Whittingham,[‡] and Rajeev Gupta*[,†]

[†]*Department of Chemistry, University of Delhi, Delhi − 110 007, India, and* [‡]*Department of Chemistry and Institute for Materials Research, State University of New York at Binghamton, Binghamton, New York 13902-6000*

Received February 3, 2009

The present work demonstrates the utilization of the Co^{3+} complex of pyridine−amide ligand as building blocks for the assembly of heterobimetallic complexes. These Co^{3+}-centered building blocks orient the tethered pyridine groups to a preorganized cleft that successively coordinates to the Cd^{2+} and Hg^{2+} ions in the periphery. Both $\{Cd^{2+}-Co^{3+}-Cd^{2+}\}$ and $\{Hg^{2+}-Co^{3+}-Hg^{2+}\}$ heterobimetallic complexes have been thoroughly characterized, including crystal structures depicting interesting weak interactions in the solid state. The $\{Cd^{2+}-Co^{3+}-Cd^{2+}\}$ and $\{Hg^{2+}-Co^{3+}-Hg^{2+}\}$ heterobimetallic complexes have been further used for the catalytic cyanosilylation of imines and ring-opening reactions of oxiranes and thiiranes. The results suggest peripheral metal-selective catalytic reactions.

Introduction

Remarkable progress has been made in the area of molecular inorganic−organic hybrid compounds. These compounds hold promise as new materials with novel catalytic, magnetic, electronic, and optical properties.[1] Versatile synthetic approaches for the assembly of such structures from *building blocks* have been developed.[2] Considerable effort has been devoted to tune the building blocks as connectors and linkers in order to reach the stage of rational design with predictable architectures.[3] Most of the literature work is centered on developing the inorganic−organic hybrid compounds consisting of nondirectional ligands coordinated to the metal ions. There are very few reports on controlling the topology of the resultant metal−ligand structure.[4] Attempts to control the dimensionality and topology of these materials depend on the judicious selection of multidentate ligands with metal ions of appropriate coordination geometry.[5]

Our approach is to design, synthesize, and utilize the coordination complexes as the building blocks for the construction of ordered structures. The benefit of a coordination complex as the building block is manifold. First, a transition

*To whom correspondence should be addressed. Fax: 91-11-2766 6605. E-mail: rgupta@chemistry.du.ac.in.

(1) (a) Kitagawa, S.; Kitaura, R.; Noro, S. *Angew. Chem., Int. Ed.* **2004**, *43*, 2334. (b) Férey, G. *Chem. Soc. Rev.* **2007**, *37*, 191. Wong-Foy, A. G.; Matzger, A. J.; Yaghi, O. M. *J. Am. Chem. Soc.* **2006**, *128*, 3494. (c) Kaye, S. S.; Dailly, A.; Yaghi, O. M.; Long, J. R. *J. Am. Chem. Soc.* **2007**, *129*, 14176. (d) Collins, D. J.; Zhou, H.-C. *J. Mater. Chem.* **2007**, *17*, 3154. (e) Yaghi, O. M.; O'Keeffe, M.; Ockwig, N. W.; Chae, H. K.; Eddaoudi, M.; Kim, J. *Nature* **2003**, *423*, 705. (f) Eddaoudi, M.; Moler, D. B.; Li, H.; Chen, B.; Reineke, T. M.; O'Keeffe, M.; Yaghi, O. M. *Acc. Chem. Res.* **2001**, *34*, 319. (g) Kitagawa, S.; Kitaura, R.; Noro, S.-I. *Angew. Chem., Int. Ed.* **2004**, *43*, 2334. (h) Koblenz, T. S.; Wassenaar, J.; Reek, J. N. H. *Chem. Soc. Rev.* **2008**, *37*, 247. (i) Delgado-Friedrich, O.; O'Keeffe, M.; Yaghi, O. M. *Phys. Chem. Chem. Phys.* **2007**, *9*, 1035. (j) Moulton, B.; Zaworotko, M. J. *Chem. Rev.* **2001**, *101*, 1629. (k) Robson, R. *J. Chem. Soc., Dalton Trans.* **2000**, 3735.

(2) (a) Fischer, R. A.; Woll, C. *Angew. Chem., Int. Ed.* **2008**, *47*, 2. (b) Kesanli, B.; Lin, W. *Coord. Chem. Rev.* **2003**, *246*, 305. (c) Reference 1. (d) Pardo, E.; Ruiz-García, R.; Cano, J.; Ottenwaelder, X.; Lescouezec, R.; Journaux, Y.; Lloret, F.; Julve, M. *Dalton Trans.* **2008**, 2780. (e) Ganguly, R.; Sreenivasulu, B.; Vittal, J. J. *Coord. Chem. Rev.* **2008**, *252*, 1027. (f) Lee, S. J.; Hupp, J. T. *Coord. Chem. Rev.* **2006**, *250*, 1710.

(3) (a) James, S. L. *Chem. Soc. Rev.* **2003**, *32*, 276. (b) Thomas, J. A. *Chem. Soc. Rev.* **2007**, *36*, 856. (c) Dalgarno, S. J.; Power, N. P.; Atwood, J. L. *Coord. Chem. Rev.* **2008**, *252*, 825. (d) Tanaka, D.; Kitagawa, S. *Chem. Mater.* **2008**, *20*, 922. (e) Das, N.; Mukherjee, P. S.; Arif, A. M.; Stang, P. J. *J. Am. Chem. Soc.* **2003**, *125*, 13950. (f) Mukherjee, P. S.; Das, N.; Stang, P. J. *J. Org. Chem.* **2004**, *69*, 3526. (g) Mukherjee, P. S.; Das, N.; Kryeschenko, Y.; Arif, A. M.; Stang, P. J. *J. Am. Chem. Soc.* **2004**, *126*, 2464.

(4) (a) Halper, S. R.; Do, L.; Stork, J. R.; Cohen, S. M. *J. Am. Chem. Soc.* **2006**, *128*, 15255. (b) Stork, J. R.; Thoi, V. S.; Cohen, S. M. *Inorg. Chem.* **2007**, *46*, 11213. Halper, S. R.; Choen, S. M. *Inorg. Chem.* **2005**, *44*, 486. (c) Halper, S. R.; Cohen, S. M. *Chem.—Eur. J.* **2003**, *9*, 4661. (d) Halper, S. R.; Cohen, S. M. *Angew. Chem., Int. Ed.* **2004**, *43*, 2385. (e) Kumar, D. K.; Jose, D. A.; Das, A.; Dastidar, P. *Inorg. Chem.* **2005**, *44*, 6933. (f) Kleij, A. W.; Reek, J. N. H. *Chem.—Eur. J.* **2006**, *12*, 4218 and references therein. (g) Kleij, A. W.; Lutz, M.; Spek, A. L.; van Leeuwen, P. W. N. M.; Reek, J. N. H. *Chem. Commun.* **2005**, 3661.

(5) (a) Seo, J. S.; Whang, D.; Lee, H.; Jun, S. I.; Oh, J.; Jeon, Y. J.; Kim, K. *Nature* **2000**, *404*, 982. (b) Aridomi, T.; Igashira-Kamiyama, A.; Konno, T. *Inorg. Chem.* **2008**, *47*, 10202. (c) Aridomi, T.; Kawamoto, T.; Konno, T. *Inorg. Chem.* **2008**, *46*, 1343. (d) Aridomi, T.; Takamura, K.; Igashira-Kamiyama, A.; Kawamoto, T.; Konno, T. *Chem.—Eur. J.* **2008**, *14*, 7752. (e) Hamilton, B. H.; Kelly, K. A.; Malasi, W.; Ziegler, C. J. *Inorg. Chem.* **2003**, *42*, 3067–3073. (f) Shin, D. M.; Lee, I. S.; Chung, Y. K.; Lah, M. S. *Inorg. Chem.* **2003**, *42*, 5459.

Published on Web 05/15/2009

metal ion induces structural rigidity in the complexes of multidentate ligands through particular coordination geometry. Such an induced rigidity has the ability to place the auxiliary functional groups in a preorganized conformation. Second, the selection of the central metal ion with a particular geometry will introduce an option to control the geometrical placement of the auxiliary functional groups.

The strategy described here uses a cobalt(III) complex of pyridine−amide ligand as a building block for next-generation heterometallic systems. The geometry of the Co(III) ion orients the tethered pyridine rings with a definite directionality to coordinate a secondary metal ion, making suitable monomeric building blocks for preparing heterobimetallic complexes. Utilizing this strategy, we have recently[6] demonstrated the use of Co^{3+} coordination complexes **1** and **2** (or **2a**) as building blocks for the preparation of $\{Co^{3+}-Zn^{2+}\}$ complex **3** and $\{Zn^{2+}-Co^{3+}-Zn^{2+}\}$ heterobimetallic complexes **4**, **4a**, and **4b** (Scheme 1). The selection of the peripheral metal ion was based on the possible application of the exposed Lewis acidic metal ion in organic transformations. Indeed, the Lewis acidic property of the peripheral Zn^{2+} ion(s) was demonstrated by the catalytic Beckmann rearrangement of the aldoximes and ketoximes, producing the corresponding amides. In order to further understand the coordinating abilities of such molecular clefts and their probability to accommodate bigger cations, we planned to further explore the studies of the remaining group 12 metal ions, cadmium and mercury. Extending this approach, we report herein the synthesis and characterization of $\{Cd^{2+}-Co^{3+}-Cd^{2+}\}$ and $\{Hg^{2+}-Co^{3+}-Hg^{2+}\}$ heterobimetallic complexes. Further, we also show the applications of these heterobimetallic complexes in a few organic transformation reactions and demonstrate the importance of the peripheral metal ions in controlling the product distribution and, in one case, regioselectivity.

Scheme 1

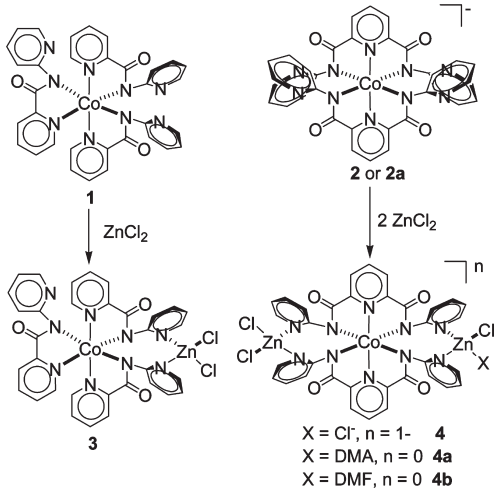

Scheme 2

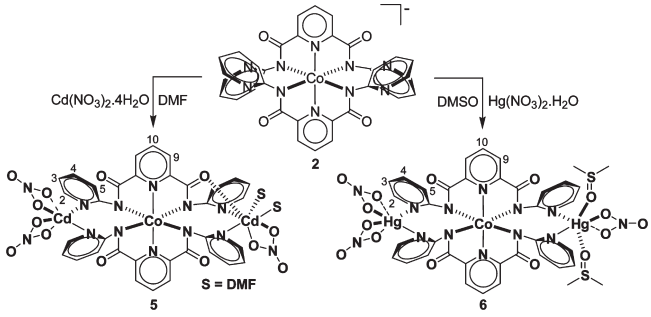

Results and Discussions

Design Criteria. The cobalt(III) complex $[Co(L)_2]^-$ (Na^+ (**2**) or Et_4N^+ (**2a**) salt) has been used as the building block in the present investigation.[6,7] In this complex, the central cobalt(III) ion is octahedrally surrounded by two pyridine−amide ligands where N_{amide} atoms constitute the N_4 basal plane and $N_{pyridine}$ atoms take the axial positions. This coordination mode of the ligand, however, leaves two tethered pyridine rings per ligand uncoordinated or *hanging*. Two such hanging pyridine rings from two ligands converge to form a *cleft* that is ideally suited to house a suitable metal ion. Our earlier study has shown that such clefts coordinate to the zinc(II) ion to afford $\{Co^{3+}-Zn^{2+}\}$ and $\{Zn^{2+}-Co^{3+}-Zn^{2+}\}$ heterobimetallic complexes (Scheme 1).[6] The coordination of the peripheral Zn(II) ions to the clefts did not result in significant structural distortion of the central Co(III) coordination core, as observed by the marginally altered bonding parameters of the $\{Zn^{2+}-Co^{3+}-Zn^{2+}\}$ complex **4a** compared to the parent complex **2a**. The enhanced stability of the Co(III)-complex-based building block and flexible nature of the tethered pyridine rings prompted us to prepare the analogous $\{Cd^{2+}-Co^{3+}-Cd^{2+}\}$ and $\{Hg^{2+}-Co^{3+}-Hg^{2+}\}$ complexes. In addition, the peripheral metal ions, Cd^{2+} and Hg^{2+}, may also show different catalytic reactions due to their bigger size and different Lewis acidic properties.

Synthesis and Properties of $\{Cd^{2+}-Co^{3+}-Cd^{2+}\}$ and $\{Hg^{2+}-Co^{3+}-Hg^{2+}\}$ Heterobimetallic Complexes. The $\{Cd^{2+}-Co^{3+}-Cd^{2+}\}$ and $\{Hg^{2+}-Co^{3+}-Hg^{2+}\}$ complexes, $[Co(L)_2-\{Cd^{2+}\}_2(NO_3)_3(DMF)_2]$ (**5**) and $[Co(L)_2-\{Hg^{2+}\}_2(NO_3)_3(DMSO)_2]$ (**6**), were synthesized by the reaction of the parent complex **2** with $M(NO_3)_2$ salt in DMF (for **5**) or DMSO (for **6**) (Scheme 2). The insertion of the peripheral metal ions immediately resulted in a distinct color change from deep green to yellow−brown. Complexes **5** and **6** were isolated as deep yellow−brown crystalline solids in 50−60% yield. The absorption spectra for **5** and **6** are quite similar to each other and composed of λ_{max} in the region of 650−660 nm, whereas other features are at ∼470 nm and below 380 nm (Figure S1, Supporting Information). The former feature may be assigned as the ligand field in nature, while the high-energy features are most likely charge-transfer in nature. The FTIR spectra of **5** and **6** clearly show the stretches for the bidentate NO_3^- ions at ∼1380 cm^{-1}, while the stretches for the coordinated DMF and DMSO appear at 1655 and 1017 cm^{-1}, respectively.[8] The conductivity measurements[9] of the freshly prepared solutions

(6) Mishra, A.; Ali, A.; Upreti, S.; Gupta, R. *Inorg. Chem.* **2008**, *47*, 154.
(7) Mishra, A.; Kaushik, N. K.; Verma, A. K.; Gupta, R. *Eur. J. Med. Chem.* **2008**, *43*, 2189.
(8) Nakamoto, K. *Infrared and Raman Spectra of Inorganic and Coordination Compounds*; Wiley: New York, **1997**.
(9) Geary, W. J. *Coord. Chem. Rev.* **1971**, *7*, 81.

of **5** and **6** do not show appreciable conductance, however, with time conductance increases suggesting partial dissociation of the NO_3^- ions.

Complexes **5** and **6** have also been characterized by NMR spectroscopy, owing to their diamagnetic state (Figures S2 and S3, Supporting Information). In general, the ^{1}H NMR spectrum of complex **5** is quite similar to those of building block **2** and $\{Zn^{2+}-Co^{3+}-Zn^{2+}\}$ complexes **4a** and **4b**.[6,7] For **5**, the peaks corresponding to the coordinated DMF were found at 2.80 and at 2.94 and 7.96 for the $-CH_3$ and $-CHO$ groups, respectively. The resonances for the central pyridine ring's H_9 and H_{10} were at 7.09 (doublet) and 8.06 (triplet) ppm, respectively. The hanging pyridine ring protons H_2, H_3, H_4, and H_5 resonate at 7.96, 6.98, 7.49, and 7.71 ppm, respectively. The H_2 and H_3 protons have suffered the maximum downfield shift (~0.3 ppm) compared to that in **2**, as expected due to their proximity to the Cd atom. The shift follows the following order: $H_2 \sim H_3 < H_4 < H_5 < H_9 < H_{10}$, wherein proton H_{10} is the least shifted. For complex **6**, the $-CH_3$ groups of the coordinated DMSO appear at 2.54 ppm, which is 0.04 ppm downfield shifted compared to the uncoordinated DMSO. As compared to complexes **4a**, **4b**, and **5** or building block **2**,[6,7] all pyridine ring protons are quite broad and shifted for complex **6**. We speculate that the large surface area of the Hg^{2+} and the possible dissociation of the coordinated NO_3^- ions in the solution might be the responsible factors (cf. conductivity measurements). It may be noted that the analogous $[Co(L)_2-\{Hg^{2+}\}_2(Cl)_3(DMSO)_2]$[10] compound shows well-resolved peaks that are in very good agreement with those of complexes **4a**, **4b**, and **5** as well as **2** and thus supports the possible dissociation of the coordinated NO_3^- ions. The ^{13}C NMR spectra of **5** and **6** unambiguously show peaks corresponding to the ligand and coordinated solvent molecules and are quite similar to that of complex **2**[7] (Figure S3, Supporting Information).

Structural Studies of $\{Cd^{2+}-Co^{3+}-Cd^{2+}\}$ and $\{Hg^{2+}-Co^{3+}-Hg^{2+}\}$ Heterobimetallic Complexes. The crystal structures of complexes **5** and **6** clearly demonstrate the coordination of the peripheral metal ions, Cd^{2+} and Hg^{2+}, to the clefts created by *hanging pyridine rings* emerging from the central Co^{3+} core (Figures 1 and 2, Tables 1−3). For both complexes, the geometry around the central Co^{3+} ion is compressed octahedral, as noted for the precursor molecule **2a**,[6] heterobimetallic $\{Zn^{2+}-Co^{3+}-Zn^{2+}\}$ complex **4a**,[6] and other examples in the literature with closely similar ligands.[11] The average $Co-N_{pyridine}$ distances for **5** (1.857 Å) and **6** (1.859 Å) are comparable to each other but, however, a little shorter than that of **2a** (1.871 Å) and **4a** (1.872 Å).[6] The average $Co-N_{amide}$ distance for **6** (1.976 Å) is ~0.02 Å longer than in **5** (1.958 Å) and **4a** (1.962 Å) but comparable to that of **2a** (1.976 Å). Two axial pyridine rings are trans to each other and make an angle of > 178° with the Co^{3+} ion, as also noted for **2a** and **4a**.[6] The distorted N_4 basal plane composed of N_{amide} groups perfectly houses the Co^{3+} ion.

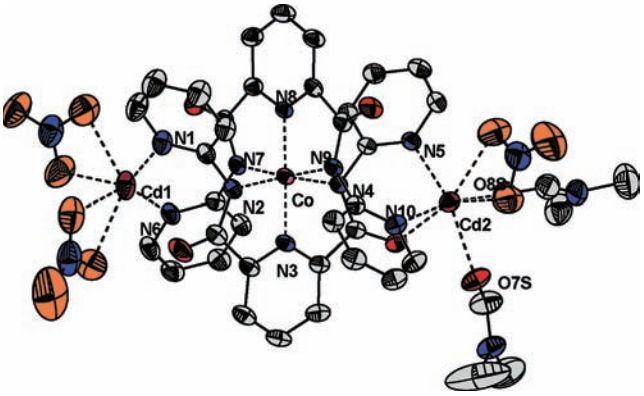

Figure 1. Molecular structure of $[Co(L)_2-\{Cd^{2+}\}_2(NO_3)_3(DMF)_2]$ (**5**) with partial numbering scheme. Thermal ellipsoids are drawn at the 30% probability level, whereas the hydrogen atoms are omitted for clarity.

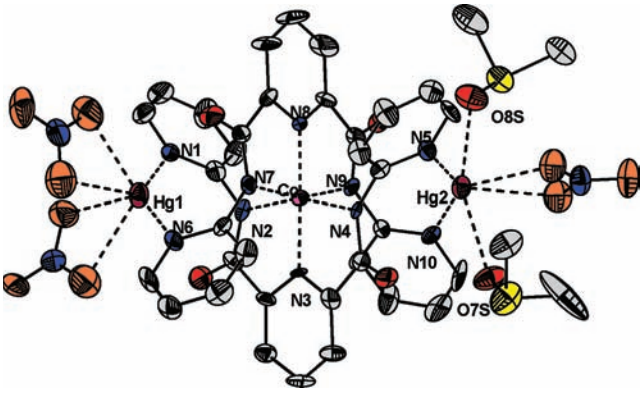

Figure 2. Molecular structure of $[Co(L)_2-\{Hg^{2+}\}_2(NO_3)_3(DMSO)_2]$ (**6**) with partial numbering scheme. Thermal ellipsoids are drawn at the 30% probability level, whereas the hydrogen atoms are omitted for clarity.

Cd1 and Hg1 are externally coordinated by two NO_3^- groups, whereas Cd2 and Hg2 have one NO_3^- and two solvent molecules. All NO_3^- groups are coordinated in bidentate fashion, where the $M-NO_3$ distances are asymmetrical in nature[12] and vary within ranges of 2.366−2.507 and 2.448−2.630 Å for complexes **5** and **6**, respectively. The $Cd-NO_3$ distances are, however, on the lower side compared to the $Hg-NO_3$ distances. It is important to mention here that, for **5**, two DMF molecules are occupying cis positions on the cadmium ion while making an angle of 82.52°. In complete contrast, two DMSO molecules are present in trans positions, making an angle of 157.7° with the Hg^{2+} ion, in **6**. It may be noted that {Co−Zn} complex **4a** has only one coordinated DMA molecule.[6] Interestingly, for the $\{Hg^{2+}-Co^{3+}-Hg^{2+}\}$ complex **6**, the sulfur atoms of the coordinated DMSO molecules are under weak interaction with the O_{amide} atoms of the coordinated ligand, two distances being 3.092 and 3.302 Å, respectively. The most probable reason for this interaction is the development of a partial positive charge on the sulfur atoms (due to the delocalization of the electron density toward the oxygen atom) that interact with O_{amide} atoms carrying a partial negative

(10) Mishra, A.; Ali, A.; Gupta, R. Unpublished results.

(11) (a) Ray, M.; Ghosh, D.; Shirin, Z.; Mukherjee, R. *Inorg. Chem.* **1997**, *36*, 3568. (b) Patra, A. K.; Mukherjee, R. *Inorg. Chem.* **1999**, *38*, 1388. (c) Singh, A. K.; Balamurugan, V.; Mukherjee, R. *Inorg. Chem.* **2003**, *42*, 6497. (d) Bricks, J. L.; Reck, G.; Rurack, K.; Schulz, B.; Spieless, M. *Supramol. Chem.* **2003**, *15*, 189.

(12) (a) Pons, J.; Garcia-Anton, J.; Jimenez, R.; Solans, X.; Font-Bardia, M.; Ros, J. *Inorg. Chem. Commun.* **2007**, *10*, 1554. (b) Cameron, A. F.; Taylor, D. W. *J. Chem. Soc., Dalton Trans.* **1972**, 1608.

Table 1. Crystallographic and Structural Refinement Data for $[Co(L)_2-\{Cd^{2+}\}_2(NO_3)_3(DMF)_2]\cdot 8/3H_2O$ (**5**) and $[Co(L)_2-\{Hg^{2+}\}_2(NO_3)_3(DMSO)_2]$ (**6**)

	$[Co(L)_2-\{Cd^{2+}\}_2(NO_3)_3(DMF)_2]\cdot 8/3H_2O$ (**5**)	$[Co(L)_2-\{Hg^{2+}\}_2(NO_3)_3(DMSO)_2]$ (**6**)
molecular formula	$C_{40}H_{36}N_{15}O_{15}Cd_2Co.8/3\ H_2O$	$C_{38}H_{34}N_{13}O_{15}S_2Hg_2Co$
fw	3879.77	1437.03
T (K)	298(2)	298(2)
cryst syst	rhombohedral	orthorhombic
space group	$R\bar{3}$	*Pbca*
a (Å)	22.953(2)	19.2666(19)
b (Å)	22.953(2)	19.0545(18)
c (Å)	22.953(2)	25.546(3)
α (deg)	110.933(1)	90
β (deg)	110.933(1)	90
γ (deg)	110.933(1)	90
V (Å^3)	8769.0(13)	9378.4(17)
Z	2	8
d (g cm^{-3})	1.469	2.036
μ/mm^{-1}	1.070	7.052
F (000)	3744	5536
goodness-of-fit (F^2)	1.159	1.130
R_1, wR_2 [$I > 2\sigma(I)$]	0.0531, 0.1754	0.0812, 0.1022
R_1, wR_2 (all data)[a]	0.0781, 0.1956	0.0958, 0.1081

[a] $R_1 = \sum||F_o| - |F_c||/\sum|F_o|$; $wR_2 = \{[\sum(|F_o|^2|F_c|^2)^2]\}^{1/2}$.

Table 2. Selected Bond Distances (Å) for $[Co(L)_2-\{Cd^{2+}\}_2(NO_3)_3(DMF)_2]$ (**5**) and $[Co(L)_2-\{Hg^{2+}\}_2(NO_3)_3(DMSO)_2]$ (**6**)

bond[a]	$[Co(L)_2-\{Cd^{2+}\}_2(NO_3)_3(DMF)_2]$ (**5**)	$[Co(L)_2-\{Hg^{2+}\}_2(NO_3)_3(DMSO)_2]$ (**6**)
Co−N2	1.947(4)	1.974(12)
Co−N3	1.853(4)	1.859(12)
Co−N4	1.967(4)	1.960(11)
Co−N7	1.963(4)	1.985(12)
Co−N8	1.860(4)	1.859(11)
Co−N9	1.956(4)	1.983(11)
M1−N1	2.216(5)	2.156(15)
M1−N6	2.267(5)	2.163(13)
M2−N5	2.288(4)	2.148(13)
M2−N10	2.396(5)	2.161(13)
M1−O1S	2.338(7)	2.46(2)
M1−O2S	2.468(9)	2.58(2)
M1−O4S	2.402(7)	2.448(18)
M1−O5S	2.368(8)	2.58(2)
M2−O2	2.463(4)	
M2−O7S	2.279(4)	2.409(16)
M2−O8S	2.335(5)	2.538(14)
M2−O9S	2.507(7)	2.630(18)
M2−O10S	2.366(6)	2.527(19)

[a] M1 and M2 stand for Cd and Hg atoms for complexes **5** and **6**, respectively.

Table 3. Selected Bond Angles (deg) for $[Co(L)_2-\{Cd^{2+}\}_2(NO_3)_3(DMF)_2]$ (**5**) and $[Co(L)_2-\{Hg^{2+}\}_2(NO_3)_3(DMSO)_2]$ (**6**)

bond angle[a]	$[Co(L)_2-\{Cd^{2+}\}_2(NO_3)_3(DMF)_2]$ (**5**)	$[Co(L)_2-\{Hg^{2+}\}_2(NO_3)_3(DMSO)_2]$ (**6**)
N2 Co N4	162.99(18)	162.3(6)
N2 Co N7	87.73(17)	92.8(5)
N2 Co N8	97.98(18)	98.2(5)
N2 Co N9	95.43(17)	89.2(5)
N3 Co N2	81.65(18)	81.6(6)
N3 Co N4	81.35(17)	80.8(5)
N3 Co N7	97.08(17)	97.1(6)
N3 Co N8	178.66(17)	178.3(6)
N3 Co N9	99.52(17)	100.4(5)
N4 Co N7	94.75(17)	90.3(5)
N4 Co N8	99.03(17)	99.5(5)
N4 Co N9	86.99(17)	93.1(5)
N7 Co N8	81.62(16)	81.3(6)
N7 Co N9	163.39(17)	162.5(5)
N8 Co N9	81.79(16)	81.2(5)
N1 M1 N6	117.66(16)	134.6(5)
N5 M2 N10	104.81(16)	135.5(5)
O7S M2 O8S	82.52(19)	157.7(6)

[a] M1 and M2 stand for Cd and Hg atoms for complexes **5** and **6**, respectively.

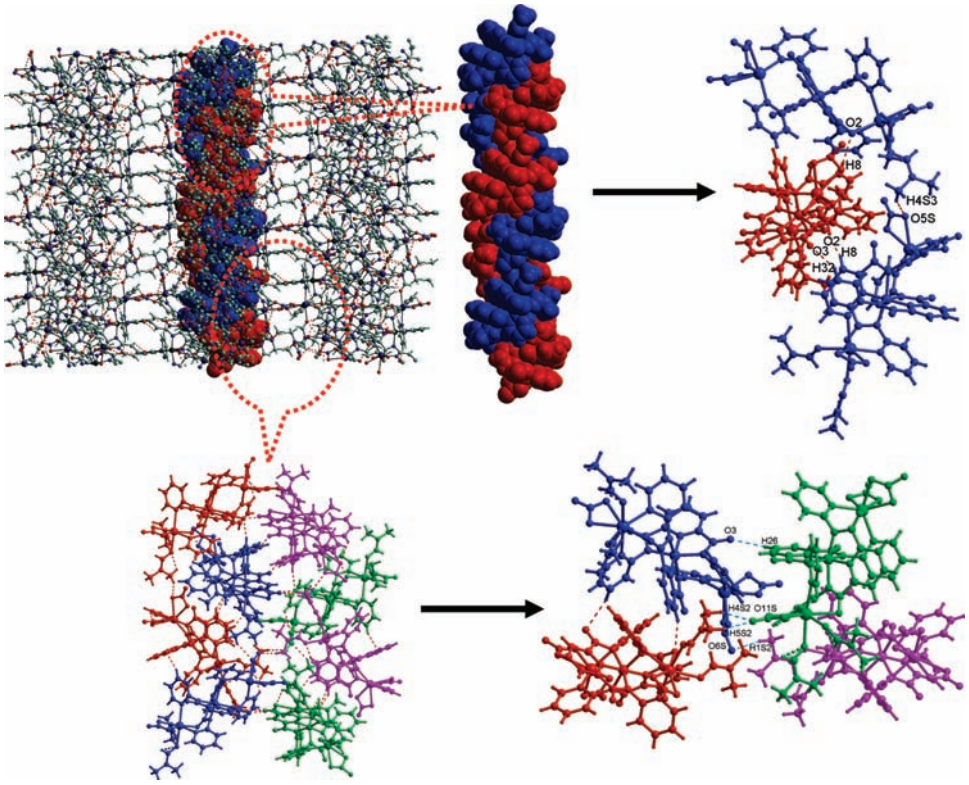

Figure 3. Extended structure of $[Co(L)_2-\{Cd^{2+}\}_2(NO_3)_3(DMF)_2]$ (**5**) showing various weak interactions and packing. See text for details.

charge. The average Cd1−$N_{pyridine}$ distance of 2.242 Å is ∼0.1 Å shorter than the Cd2−$N_{pyridine}$ distance, whereas for analogous mercury complex **6**, these distances are comparable (2.160 and 2.155 Å, respectively). Further, Cd2 is also coordinated by the O_{amide} (2.463 Å) from the attached ligand, completing a distorted seven-coordinate geometry around the cadmium ion. The other cadmium ion remains six-coordinate, whereas for **6**, both Hg^{2+} ions are six−coordinate in nature as well. In the case of **5**, the difference in the Cd−$N_{pyridine}$ distance is most likely due to the difference in the number of ligands attached to two Cd ions. We observed a similar trend for the respective Cd−NO_3 distances as well. For complex **4a**, the difference of ∼0.04 Å in the average Zn1−$N_{pyridine}$ (2.064 Å) and Zn2−$N_{pyridine}$ (2.029 Å) distances was attributed to the difference in the number of attached anionic ligands.[6] The average Cd−$N_{pyridine}$ and Hg−$N_{pyridine}$ distances are on the lower side compared to literature examples.[12,13] The Cd−DMF as well as the Hg−DMSO distances are within the range observed in other structurally characterized complexes.[14] The hanging pyridine rings make an angle of ∼135° both with Hg1 and Hg2 ions, whereas the respective angles are ∼118° and ∼105° for Cd1 and Cd2 ions, respectively. Clearly, the additional coordination of the O_{amide} to the Cd2 ion has tilted one of the hanging pyridine rings, which resulted in a smaller bite angle. For comparison, the N−Zn−N angles for the analogous $\{Zn^{2+}-Co^{3+}-Zn^{2+}\}$ complex **4a** were 122.1° and 127.3° for Zn1 and Zn2 ions, respectively.[6]

Weak Interactions. Complexes **5** and **6** display various weak interactions in the solid state, resulting in interesting packing behavior. Careful examination of the crystal structure demonstrates a unique supramolecular organization in complexes **5** and **6** (Figures 3 and 4; Table S1, Supporting Information). In **5**, the individual molecules are stitched together in an interesting fashion where weak C−H···O H−bonding interactions are playing a significant role in forming a unique supramolecular packing (Figure 3). H-bonding interactions via $C4S_{DMF}$−H4S3···$O5S_{nitrate}$ (2.171(13) Å) lead to the formation of a 1-D chain along [111]. These chains are further linked via $O3_{amide}$···H32−$C32_{pyridine}$ (2.499(6) Å), $O2_{amide}$···H8−$C8_{pyridine}$ (2.175(5) Å), and $C8_{pyridine}$−H8···$O2_{amide}$ (2.175(5) Å) H bonds to form an interesting double-helical strand. This H−bonding scheme becomes more obvious by the fact that each such moiety is further linked to the four crystallographically equivalent adjacent units (shown in four different colors, Figure 3) via $C26_{pyridine}$−H26···$O3_{amide}$ (2.444(7) Å), $C1S_{DMF}$−H1S2···$O6S_{nitrate}$ (2.411(96) Å), $C4S_{DMF}$−H4S2···$O11S_{nitrate}$ (2.430(16) Å), and $C5S_{DMF}$−H5S2···$O11S_{nitrate}$ (2.435(16) Å) and turns into a double-helical strand. In the crystal lattice, these helical strands are stacked one over the other perpendicular to the *c* axis, which is repeatedly connected through weak C−H···O bonds to form a complex 3-D supramolecular network. The formation of supramolecular helical strands appears to be a combination of weak C−H···O interactions along with crystal packing effects.

In a manner similar to that of complex **5**, the crystal structure of **6** also demonstrates a unique supramolecular

(13) (a) Mendoza-Diaz, G.; Rigotti, G.; Piro, O. E.; Sileo, E. E. *Polyhedron* **2005**, *24*, 777. (b) Kang, D.; Seo, J.; Lee, S. Y.; Lee, J. Y.; Choi, K. S.; Lee, S. S. *Inorg. Chem. Commun.* **2007**, *10*, 1425. (c) March, R.; Pons, J.; Ros, J.; Clegg, W.; Alvarez-Larena, A.; Piniella, J. F.; Sanz, J. *Inorg. Chem.* **2003**, *42*, 7403.

(14) Burrows, A. D.; Cassar, K.; Duren, T.; Friend, R. M. W.; Mahon, M. F.; Rigby, S. P.; Savarese, T. L. *Dalton Trans.* **2008**, 2465.

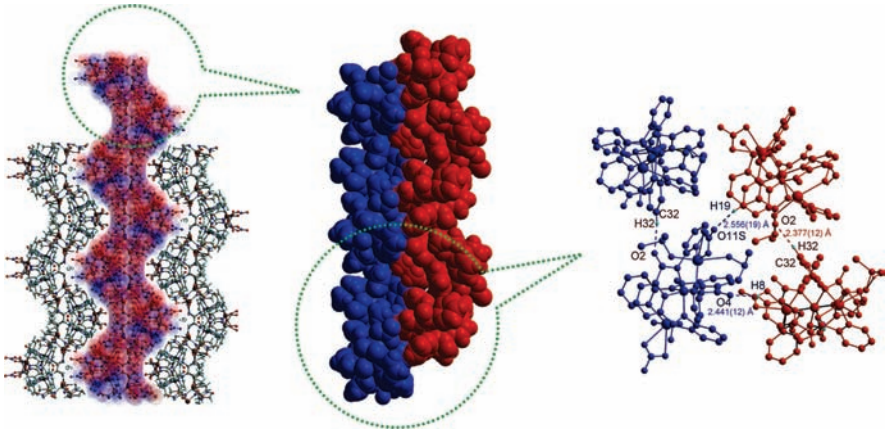

Figure 4. Extended structure of $[Co(L)_2-\{Hg^{2+}\}_2(NO_3)_3(DMSO)_2]$ (**6**) showing various weak interactions and packing. See text for details.

organization manifested by various weak C−H···O interactions (Figure 4; Table S1, Supporting Information). Interestingly, each molecule provides six nonbonding sites of three donors ($C8_{pyridine}$−H8, $C19_{pyridine}$−H19, and $C32_{pyridine}$−H32) and three acceptors ($O4_{amide}$, $O11S_{nitrate}$, and $O2_{amide}$) that participate in the C−H···O interactions. Each complex is further connected to three similar adjacent moieties (shown in different colors, Figure 4) owing to the occurrence of C−H···O interactions. It was observed that C32−H32···O2 (2.377 (12) Å) is connected to two neighboring moieties along [100]. However, other two sites (C8−H8···O4 (2.441(12) Å) and C19−H19···O11S (2.556(19) Å) are further connected in a cross-intermolecular fashion to create a sinusoidal 1-D helical strand (Figure 4). In the crystal lattice, these helical strands lie on the *ab* plane. The helical chain escalation is further assisted via C32−H32···O2 and O2···H32−C32 interactions, consecutively, and, hence, play a central role in stabilizing the 1-D supramolecular helical strands. Several intramolecular H-binding interactions and steric hindrances cape the other active outlets within the molecule and confine the possibility of limited active intermolecular sites,; therefore, such strands are uniformly distributed in the crystal lattice.

Organic Transformation Reactions. The availability of the Lewis acidic metal ions in the periphery of the heterobimetallic complexes, $\{M^{2+}-Co^{3+}-M^{2+}\}$ (M = Zn^{2+}, **4b**; Cd^{2+}, **5**; and Hg^{2+}, **6**), offers an excellent opportunity to carry out comparative catalytic studies involving various substrates. The relative size and Lewis acidic property of the catalytic peripheral metal ion may play an important and decisive role in product distribution and selectivity. In addition, the preferential binding/interaction of the substrate and nucleophile to/with the catalytic metal ion may also facilitate the reaction between two components. The importance of the Lewis acidic metals in metal−organic frameworks (MOFs) and other similar interesting structures has recently gained attention because they can be used as catalysts for various organic transformations.[15] The selected studies include regio- and enantioselective catalysis[15b−15g] as well as size- and shape-selective catalysis.[15a] However, most of the literature examples use complicated multistep design for the construction of such catalysts, whereas the high catalyst loading and non-reusability of the active catalysts limits the scope of such reactions.[16] The heterobimetallic catalysts described in this work are shown to catalyze various organic transformations using a small catalyst loading at room temperature. These reactions are fast and clean, with no further purification required in most of the cases. In addition, the catalysts can be recovered after the reaction and reused several times (tested five times) without a significant loss of activity. We selected cyanation of imines and ring-opening reactions of the oxiranes and thiiranes due to the proposed involvement of a Lewis acid in these catalytic transformation reactions.

1. Strecker Reaction. The Strecker reaction or the cyanation of imines is a simple and efficient method for the synthesis of α-aminonitriles, which are important precursors for the synthesis of α-amino acids and other nitrogen-containing heterocycles.[17] Classically, the Strecker reaction is carried out by the nucleophilic addition of a cyanide ion to the imines using catalysts.[18] The activation of the C=N bond to generate the iminium cation or the equivalent species is a prerequisite for this reaction.[19] Such an activation has been achieved by using

(15) (a) Horike, S.; Dinca, M.; Tamaki, K.; Long, J. R. *J. Am. Chem. Soc.* **2008**, *130*, 5854. (b) Wu, C.-D.; Hu, A.; Zhang, L.; Lin, W. *J. Am. Chem. Soc.* **2005**, *127*, 8940. (c) Tanaka, K.; Oda, S.; Shiro, M. *Chem. Commun.* **2008**, 820. (d) Park, J.; Lang, K.; Abboud, K. A.; Hong, S. *J. Am. Chem. Soc.* **2008**, *130*, 16484. (e) Lee, S. J.; Lin, W. *J. Am. Chem. Soc.* **2002**, *124*, 4554. (f) Ohmori, O.; Fujita, M. *Chem. Commun.* **2004**, 1586. (g) Fujita, M.; Kwon, Y. J.; Washizu, S.; Ogura, K. *J. Am. Chem. Soc.* **1994**, *116*, 1151. (h) Dewa, T.; Saiki, T.; Aoyama, Y. *J. Am. Chem. Soc.* **2001**, *123*, 502. (i) Endo, K.; Koike, T.; Sawaki, T.; Hayashida, O.; Masuda, H.; Aoyama, Y. *J. Am. Chem. Soc.* **1997**, *119*, 4117. (j) Evans, O. R.; Ngo, H. L.; Lin, W. *J. Am. Chem. Soc.* **2001**, *123*, 10395. (k) Gomez-Lor, B.; Gutierrez-Puebla, E.; Iglesias, M.; Monge, M. A.; Ruiz-Valero, C.; Snejko, N. *Inorg. Chem.* **2002**, *41*, 2429. (l) Jiang, D.; Mallat, T.; Krumeich, F.; Baiker, A. *J. Catal.* **2008**, *257*, 390.

(16) Fan, Q. H.; Li, Y.-M.; Chan, A. S. *Chem. Rev.* **2002**, *102*, 3385.

(17) (a) Williams, R. M. *Synthesis of Optically Active* α*-Amino Acids*; Pergamon: Oxford, U.K., **1989**.(b) Synthesis of α-Amino Acids, Tetrahedron Symposia in Print: O'Donell, M. J. *Tetrahedron* **1988**, *44*, 5253.

(18) (a) Groger, H. *Chem. Rev.* **2003**, *103*, 2795. (b) Prasad, B. A. B.; Bisai, A.; Singh, V. K. *Tetrahedron Lett.* **2004**, *45*, 9565. (c) Fossey, J. S.; Richards, C. J. *Tetrahedron Lett.* **2003**, *44*, 8773. (d) Takahashi, E.; Fujisawa, H.; Yanai, T.; Mukaiyama, T. *Chem. Lett.* **2005**, *34*, 318.

(19) (a) Yraguchi, D.; Terada, M. *J. Am. Chem. Soc.* **2004**, *126*, 5356. (b) Soeta, T.; Nagai, K.; Fujihara, H.; Kuriyama, M.; Tomioka, K. *J. Org. Chem.* **2003**, *68*, 9723. (c) Fernandes, R. A.; Stimac, A.; Yamamoto, Y. *J. Am. Chem. Soc.* **2003**, *125*, 14133. (d) Cogan, D. A.; Liu, G.; Ellman, J. *Tetrahedron* **1999**, *55*, 8883. (e) Masumoto, S.; Usuda, H.; Suzuki, M.; Kanai, M.; Shibasaki, M. *J. Am. Chem. Soc.* **2003**, *125*, 5634. (f) Uyehara, T.; Suzuki, I.; Yamamoto, Y. *Tetrahedron Lett.* **1989**, *30*, 4275.

different Lewis acids such as $RuCl_3$, $ZnCl_2$, $NiCl_2$, $BiCl_3$, $LiClO_4$, $VO(OTf)_2$, $Ga(OTf)_3$, $Yb(OTf)_3$, $Sc(OTf)_3$, Ln $(O^iPr)_3$ (Ln = Gd and Sm), and so forth.[20] Most of these methods require the use of strong acidic and harsh conditions, expensive reagents, and extended reaction times and lead to several byproducts and toxic waste. Few intriguing methods such as application of β-cyclodextrin,[21] ionic liquids,[22] and clays[23] have also appeared in the literature. Our catalytic conditions only required 2% catalyst loading at room temperature for the transformation. In particular, when 2 mol % of complex **5** was used as a catalyst with the mixture of imine and trimethylsilyl cyanide (TMSCN) in THF at room temperature, 80−95% of the corresponding products were isolated (Table 4). A variety of substrates were tested, and the results indicate the general nature of this reaction. A number of solvents with variable polarity were also tested for this reaction. While the reaction followed a heterogeneous pathway in THF with an ease of purification by simple filtration and a decent yield (>80%), the use of DMF resulted in a homogeneous reaction with a better yield (>90). The use of CH_3CN also resulted in comparable yield (~90%) to that of THF, even though the reaction was homogeneous in nature. The catalytic activity of complex **5** for this Strecker reaction is established by the fact that no reaction was observed in the absence of **5**. The effect of the electron-withdrawing group at the para position[21,24] of the phenyl group is clearly seen by the enhancement in the yield of the reaction; for example, the yields are 80 and 95% for $-OCH_3$ and $-F$ groups, respectively. These catalytic reactions were also tested with the analogous Hg complex **6**; interestingly, very little transformation took place (<5% by GC). We believe that the availability of the labile solvent molecules at the cis position on $\{Cd^{2+}-Co^{3+}-Cd^{2+}\}$ complex **5** provides accessibility to the substrate as well as the nucleophile (CN^-) to interact in a concomitant manner. The $\{Hg^{2+}-Co^{3+}-Hg^{2+}\}$ complex **6**, on the other hand, has a trans arrangement of the solvent molecules; therefore, a concomitant internal CN^- transfer to the substrate may not be feasible. Shibasaki et al. have also suggested a mechanism where a Lewis acidic lanthanide metal ion not only activates the imine substrate but also helps in stabilizing the nucleophile for an internal CN^- transfer to the substrate.[25] Further, the $\{Zn^{2+}-Co^{3+}-Zn^{2+}\}$ complex **4b** was also found to be almost ineffective. This can be rationalized by the fact that only one labile site is available, and a concomitant internal CN^- transfer to the substrate may not be possible.

Table 4. Strecker Reaction of Imine with TMSCN Using Catalysts **4b**, **5**, and **6**

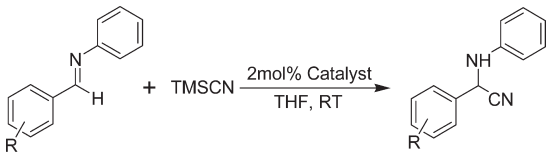

			yield[a]		
s. no.	R	time (h)	**4b**	**5**	**6**
1	H	4	trace[b]	85, 92,[c] 90[d]	<5[b,e]
2	Me	4	trace[b]	85	<5[b,e]
3	F	4	trace[b]	95, 95,[c] 88[d]	<5[b,e]
4	Cl	4	trace[b]	95, 92,[c] 86[d]	<5[b,e]
5	OMe	4	trace[b]	80	<5[b,e]
6	NO_2	4	trace[b]	90	<5[b,e]

[a] Isolated yield. [b] Remainder of mass balance was the unreacted imine. [c] The reaction was done in DMF. [d] The reaction was performed in CH_3CN. [e] Determined by the gas chromatography.

2. Ring-Opening Reactions of Epoxides and Thiiranes. Ring-opening reactions of the oxiranes (epoxides) and thiiranes with various nucleophiles are attractive due to applications in the synthesis of pharmaceutically and industrially important compounds.[26] A variety of important products could be synthesized by varying the nucleophile in such ring-opening reactions. Several methods have been reported for the ring-opening reaction of epoxides using metal amides,[27] metal salts,[28] metal alkoxides,[29] metal triflates,[30] and metal halides.[31] Compared to well-studied ring-opening reactions of the epoxides, similar reactions involving thiiranes are scarce[32] due to fast polymerization of the thiiranes and poor yield of the products.[32a] Thus, there is a need for a widely applicable approach where a common catalyst could perform ring-opening reactions of both oxiranes and thiiranes. In this

(20) (a) Heydari, A.; Fatemi, P.; Alizadesh, A.-A. *Tetrahedron Lett*. **1998**, *39*, 3049. (b) Kobayashi, S.; Nagayama, S.; Busujima, T. *Tetrahedron Lett*. **1996**, *37*, 9221. (c) De, S. K.; Gibbs, R. A. *J. Mol. Catal. A: Chem*. **2005**, *232*, 123. (d) De, S. K. *J. Mol. Catal. A: Chem*. **2005**, *225*, 169. (e) De, S. K.; Gibbs, R. A. *Tetrahedron Lett*. **2004**, *45*, 7407. (f) Mulzer, J.; Meier, A.; Buschmann, J.; Luger, P. *Synthesis* **1996**, 123. (g) De, S. K. *Synth. Commun*. **2005**, *35*, 653. (h) Kobayashi, S.; Ishitani, H.; Ueno, M. *Synlett*. **1997**, 115.

(21) Surendra, K.; Krishnaveni, N. S.; Mahesh, A.; Rama Rao, K. *J. Org. Chem*. **2006**, *71*, 2532.

(22) Yadav, J. S.; Reddy, B. V. S.; Eshwaraiah, B.; Srinivas, M.; Vishnumurthy, P. *New. J. Chem*. **2003**, *27*, 462.

(23) Yadav, J. S.; Reddy, B. V. S.; Eswaraiah, B.; Srinivas, B. *Tetrahedron* **2004**, *60*, 1767.

(24) Fukuda, Y.; Maeda, Y.; Kondo, K.; Aoyama, T. *Synthesis* **2006**, 1937.

(25) (a) Masumoto, S.; Usuda, H.; Suzuki, M.; Kanai, M.; Shibasaki, M. *J. Am. Chem. Soc*. **2003**, *125*, 5634. (b) Takamura, M.; Hamashima, Y.; Usuda, H.; Kanai, M.; Shibasaki, M. *Chem. Pharm. Bull*. **2000**, *48*, 1586.

(26) (a) Connolly, M. E.; Kersting, F.; Bollery, C. T. *Prog. Cardiovasc. Dis*. **1976**, *19*, 203. (b) Triggle, D. J. In *Burger's Medicinal Chemistry*, 4th ed; Wolff, M. S., Ed.; Wiley-Interscience: New York, **1981**; p 225. (c) De Cree, J.; Geukens, H.; Leempoels, J.; Verhaegen, H. *Drug Delivery Res*. **1986**, *8*, 109. (d) Young, R. R.; Gowen, J. H.; Shahani, B. T. *N. Engl. J. Med*. **1975**, *293*, 950. (e) Joossens, J.; Vander-Veken, P.; Lambeir, A. M.; Augustyns, K.; Haemers, A. *J. Med. Chem*. **2004**, *47*, 2411.

(27) Yamada, J.; Yumoto, M.; Yamamoto, Y. *Tetrahedron Lett*. **1989**, *30*, 4255.

(28) (a) Zhao, P. Q.; Xu, L. W.; Xia, C. G. *Synlett* **2004**, 846. (b) Kamal, A.; Ramu, R.; Azhar, M. A.; Khanna, G. B. R. *Tetrahedron Lett*. **2005**, *46*, 2675.

(29) Sagawa, S.; Abe, H.; Hase, Y.; Inaba, T. *J. Org. Chem*. **1999**, *64*, 4962.

(30) (a) Auge, J.; Leroy, F. *Tetrahedron Lett*. **1996**, *37*, 7715. (b) Chini, M.; Crotti, P.; Favero, L.; Macchia, M.; Pineschi, M. *Tetrahedron Lett*. **1994**, *35*, 433. (c) Meguro, M.; Asao, N.; Yamamoto, Y. *J. Chem. Soc., Perkin Trans. 1* **1994**, 2597.(d) Ollevier, T.; Lavie-Compin, G. *Tetrahedron Lett*. **2004**, *45*, 49.

(31) (a) Reddy, L. R.; Reddy, M. A.; Bhanumati, N.; Rao, K. R. *Synthesis* **2001**, 831. (b) Chakraborti, A. K.; Kondaskar, A. *Tetrahedron Lett*. **2003**, *44*, 8315.

(32) (a) Sander, M. *Chem. Rev*. **1966**, *66*, 297. (b) Dong, Q.; Fang, X.; Schroeder, J. D.; Garvey, D. S. *Synthesis* **1999**, 1106. (c) Reddy, M. S.; Surendra, K.; Krishnaveni, S.; Narender, M.; Rama Rao, K. *Helv. Chim. Acta* **2007**, *90*, 337. (d) Takeuchi, H.; Nakajima, Y. *J. Chem. Soc., Perkin Trans. 2* **1998**, 2441.

Table 5. Ring-Opening Reaction of the Cyclohexene Oxide with Aniline and p-Substituted Anilines Using Catalysts **4b**, **5**, and **6**

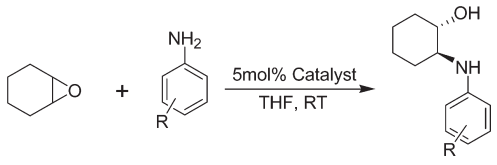

			yield[a]		
s. no.	R	time (h)	**4b**	**5**	**6**
1	H	8	65, 65,[b] 62[c]	80, 77,[b] 74[c]	60, 57,[b] 57[c]
2	Me	8	65	80	60
3	Cl	8	55	77	55
4	OMe	8	65	90	62
5	NO_2	16	10	20	5

[a] Isolated yield. [b] Third run with reused catalyst. [c] Fifth run with reused catalyst.

context, the $\{M^{2+}-Co^{3+}-M^{2+}\}$ ($M = Zn^{2+}$, **4b**; Cd^{2+}, **5**; and Hg^{2+}, **6**) heterobimetallic complexes offer an excellent opportunity to carry out comparative catalytic studies involving various epoxides and thiiranes. The relative size and Lewis acidic property of the catalytic peripheral metal ion may play an important role in the ring-opening reactions. In addition, the preferential binding of the substrate (oxiranes versus thiiranes) toward catalytic metal atoms may also facilitate the ring-opening reaction.

To find the most effective catalyst, the cyclohexene oxide was treated with aniline or para-substituted aniline in the presence of 5 mol % of the catalyst, and the results are summarized in Table 5. The reactions were monitored by thin-layer chromatography and gas chromatography mass spectrometry (GCMS); however, the products were isolated and characterized in all cases. In each case, trans-2-phenylaminocyclohexanol was formed as the sole product. All three $\{M^{2+}-Co^{3+}-M^{2+}\}$ catalysts (M = Zn, Cd, and Hg) were tested; however, the reaction was best catalyzed by the $\{Cd^{2+}-Co^{3+}-Cd^{2+}\}$ complex **5** with high conversion. The applicability of three catalysts was evaluated for the aminolysis of cyclohexene oxide with various p-substituted anilines. The yields were higher with the electron-rich anilines (entries 2 and 4, Table 5) due to the better nucleophilicity of the substituted amine. For example, with the Cd catalyst, the yield dropped from 90% to only 20% by introducing $-NO_2$ in place of the $-OCH_3$ group. A similar trend has also been observed in the literature.[33,34] Next, the ring-opening reactions of the thiiranes were attempted, and the results are documented in Table 6. When the cyclohexene sulfide was treated with aniline, analogous trans-2-phenylaminocyclohexanethiol was formed in good yield. As observed for the cyclohexene oxide, the product yield was on the higher side with electron-donating groups at the para position of the aniline.[33,34] Interestingly, isolated yields are higher with the Hg catalysts, **6**, than the analogous Zn or Cd catalysts,

Table 6. Ring-Opening Reaction of the Cyclohexene Sulfide with Aniline and p-Substituted Anilines Using Catalysts **4b**, **5**, and **6**

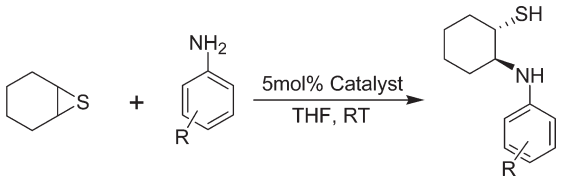

			yield[a]		
s. no.	R	time (h)	**4b**	**5**	**6**
1	H	12	65, 62,[b] 62[c]	65, 63,[b] 62[c]	80, 80,[b] 77[c]
2	Me	12	70	70	82
3	Cl	12	62	62	75
4	OMe	12	70	70	85
5	NO_2	24	5	5	20

[a] Isolated yield. [b] Third run with reused catalyst. [c] Fifth run with reused catalyst.

Table 7. Ring-Opening Reaction of the Styrene Oxide with Aniline and p-Substituted Anilines Using Catalysts **4b**, **5**, and **6**

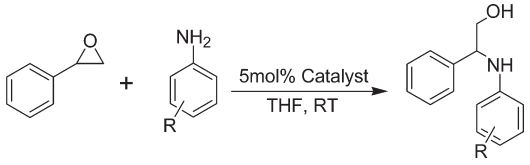

			yield[a]		
s. no.	R	time (h)	**4b**	**5**	**6**
1	H	8	75, 72,[b] 70[c]	85, 85,[b] 82[c]	70, 65,[b] 62[c]
2	Me	8	75	85	65
3	Cl	8	65	80	60
4	OMe	8	75	90	70
5	NO_2	16	25	40	15

[a] Isolated yield. [b] Third run with reused catalyst. [c] Fifth run with reused catalyst.

4b and **5**, respectively. We believe that the strong affinity of the mercury(II) ion to interaction with the softer sulfur atom is the primary reason. This Hg···S interaction activates the thiiarane ring more effectively and enables the ring-opening reaction in an efficient manner.

To determine the regioselectivity, styrene oxide was used as a representative unsymmetrical epoxide[33,34] and was treated with aniline or p-substituted aniline in the presence of 5 mol % of the catalyst (Table 7). Interestingly, a perfect regioselectivity was observed that resulted in only a single product in all cases with all three catalysts. Out of two possible products due to the nucleophilic attack either at the benzylic carbon atom or at the less-hindered carbon atom of the epoxide ring, in all cases, nucleophilic attack took place at the benzylic carbon atom of the epoxide.[33] The regio-isomer formed by the reaction of the amine at the benzylic carbon atom of the epoxide ring showed the characteristic molecular ion peak at m/z [$M^+ - 31$] due to the loss of the CH_2OH

(33) Shivani, Pujala, B.; Chakraborti, A. K. *J. Org. Chem.* **2007**, *72*, 3713.
(34) Mancilla, G.; Femenia-Rios, M.; Macias-Sanchez, J.; Collado, I. G. *Tetrahedron* **2008**, *64*, 11732.

fragment in the GCMS studies.[33] This conclusively proves a single product, as the other regioisomer is expected to show an ion peak at m/z [$M^+ - 107$] due to the loss of the C_6H_5CHOH fragment for the product formed by the reaction at the terminal carbon atom of the epoxide ring.[33] The results indicate that the epoxide ring has interacted with the peripheral metal atom (Zn, Cd, or Hg) through the less-hindered side, possibly due to steric reasons. The isolated yields are again higher for the $\{Cd^{2+}-Co^{3+}-Cd^{2+}\}$ catalyst **5** as also observed for cyclohexene oxide. We speculate that the presence of cis labile sites on the cadmium ion and the right match of size and Lewis acidic property are the predominant factors.

Conclusion

We have demonstrated the utilization of a Co^{3+} complex as the building block for the assembly of $\{Cd^{2+}-Co^{3+}-Cd^{2+}\}$ and $\{Hg^{2+}-Co^{3+}-Hg^{2+}\}$ heterobimetallic complexes. The Co^{3+}-centered building block orients the tethered pyridine groups to a preorganized cleft that nicely accommodates Cd^{2+} and Hg^{2+} ions. Both $\{Cd^{2+}-Co^{3+}-Cd^{2+}\}$ and $\{Hg^{2+}-Co^{3+}-Hg^{2+}\}$ heterobimetallic complexes have been thoroughly characterized, including crystal structures depicting interesting weak interactions in the solid state. The $\{Cd^{2+}-Co^{3+}-Cd^{2+}\}$ and $\{Hg^{2+}-Co^{3+}-Hg^{2+}\}$ heterobimetallic complexes have been used for catalytic organic transformation reactions, and the results are further compared with that of the $\{Zn^{2+}-Co^{3+}-Zn^{2+}\}$ complex.[6] The comparative studies suggest peripheral metal-selective catalytic reactions where regioselectivity has been observed in most cases. Further studies are in progress to understand the role of the central metal (i) in the placement of the hanging pyridine rings to control cleft creation, and (ii) on the catalytic performance of the peripheral metal ions.

Experimental Section

All reagents were obtained from the commercial sources and used as received. Solvents were dried or purified as reported earlier.[6,35] The complexes $Na[Co(L)_2]$ (**2**) and $Et_4N[Co(L)_2]$ (**2a**) were synthesized according to our recent report.[7] Various organic substrates were prepared from the standard literature procedures, whereas the products were characterized by a comparison of their melting points, IR spectra, and ^1H NMR spectra with those of authentic samples. In few cases, however, GCMS studies were used for the complete characterization of the product.

Synthesis of $[Co(L)_2-\{Cd^{2+}\}_2(NO_3)_3(DMF)_2]$ (5). To a solution of $Cd(NO_3)_2\cdot 4H_2O$ (0.090 g, 0.30 mmol) in DMF (5 mL) was added a DMF solution (5 mL) of $Na[Co(L)_2]$ (**2**) (0.100 g, 0.14 mmol). After the reaction mixture was stirred for 1 h, the filtrate was subjected to diethyl ether diffusion. This afforded the deep yellow crystalline compound within 2 days. Yield: 0.075 g (43%). Anal. calcd for $C_{40}H_{36}N_{15}O_{15}CoCd_2$: C, 38.38; H, 2.87; N, 16.79. Found: C, 37.90; H, 3.15; N, 17.10. FTIR spectrum (KBr, ν, selected peaks): 1655 (DMF); 1617, 1600 (C=O); and 1384 (NO_3^-) cm^{-1}. Conductivity (DMF, ~1 mM solution at 298 K): $\Lambda_M = 20\ \Omega\ cm^2\ mol^{-1}$. Absorption spectrum [$\lambda_{max}$, nm, DMF ($\varepsilon$, $M^{-1}\ cm^{-1}$)]: 650 (10), 470 (sh, 1185), 450 (sh, 1390), 380 nm (sh, 4300). ^1H NMR spectrum [DMSO-d_6, 300 MHz, 25 °C, TMS]: δ 7.96 (*d*, 4H; br, H_2), 6.97 (m, 4H; br, H_3), 7.48 (m, 4H; br, H_4), 7.71 (*d*, 4H; H_5), 7.08 (*d*, 4H; H_9), 8.06 (*t*, 2H; H_{10}), 2.94 (CH_3, DMF), 2.80 (CH_3, DMF), 7.96 (CHO, DMF). ^{13}C NMR spectrum [DMSO-d_6, 300 MHz, 25 °C, TMS]: δ 147.98 (C_2), 122.59 (C_3), 123.29 (C_4), 119.30 (C_5), 156.18 (C_6), 167.65 (C_7), 158.79 (C_8), 137.42 (C_9), 139.73 (C_{10}), 30.76 (CH_3, DMF), 35.77 (CH_3, DMF), 162.34 (CHO, DMF).

Synthesis of $[Co(L)_2-\{Hg^{2+}\}_2(NO_3)_3(DMSO)_2]$ (6). This compound was synthesized following the procedure of **5** with following reagents: $Na[Co(L)_2]$ (**2**) (0.100 g, 0.14 mmol), $Hg(NO_3)_2\cdot H_2O$ (0.100 g, 0.29 mmol), and DMSO (10 mL). A deep yellow crystalline compound was isolated within a day. Yield: 0.070 g (35%). Anal. calcd for $C_{38}H_{34}N_{13}O_{15}S_2CoHg_2$: C, 31.75; H, 2.36; N, 12.67. Found: C, 31.40; H, 2.55; N, 12.28. FTIR spectrum (KBr, ν, selected peaks): 1614 and 1562 (C=O); 1386 (NO_3^-); 1017 (DMSO) cm^{-1}. Conductivity (DMF, ~ 1 mM solution at 298K): $\Lambda_M = 8\ \Omega^{-1}\ cm^2\ mol^{-1}$. Absorption spectrum [$\lambda_{max}$, nm, DMSO ($\varepsilon$, $M^{-1}\ cm^{-1}$)]: 660 (15), 470 (sh, 2100), 413 (sh, 3650), 330 nm (sh, 16300). ^1H NMR spectrum [DMSO-d_6, 400 MHz, 25 °C, TMS]: δ 8.21 (4H; br, H_2), 7.10 (4H; br, H_3), 7.98 (4H; br, H_4), 8.05 (4H; br, H_5), 7.61 (4H; br, H_9), 8.28 (*t*, 2H; H_{10}), 2.54 (CH_3, DMSO). ^{13}C NMR spectrum [DMSO-d_6, 300 MHz, 25 °C, TMS]: δ 147.49 (C_2), 122.41 (C_3), 123.06 (C_4), 119.18 (C_5), 156.01 (C_6), 167.45 (C_7), 158.32 (C_8), 137.32 (C_9), 139.41 (C_{10}), 38.95 (CH_3, DMSO).

General Procedure for the Cyanosilylation Reaction. The catalyst (2 mol %) was put in a dry round-bottom flask and dissolved in THF (6 vol) under a N_2 atmosphere. The respective imine (50 mg, 0.27 mmol, 1.0 equiv) was gradually added to the reaction mixture at room temperature and stirred for 15 min, followed by the dropwise addition of TMSCN (37 μL, 0.27 mmol, 1.0 equiv). The reaction mixture was further stirred for 4 h at room temperature. The progress of the reaction was monitored by TLC (10% EtOAc/hexanes). After complete consumption of the imine, the volume of the reaction mixture was concentrated under reduced pressure, and the residue was triturated with diethyl ether. The catalyst thus separated was filtered and dried. The ether layer was concentrated to give the crude product, which was purified by gradient column chromatography using 60−120 mesh silica and EtOAc/hexane as the eluent. The recovered catalyst was used for further experiments without any regeneration.

General Procedure for the Ring-Opening Reactions of Epoxides and Thiiranes. The catalyst (5 mol %) was put in a dry round-bottom flask and dissolved in THF (6 vol) under a N_2 atmosphere. The epoxide or thiirane (50 μL, 0.43 mmol, 1.0 equiv) was gradually added to the reaction mixture and stirred for 10 min, followed by the addition of aromatic amine (40 μL, 0.43 mmol, 1.0 equiv). The reaction mixture was further stirred for several hours at room temperature (as mentioned in Tables 5−7). The progress of the reaction was monitored by TLC (20% EtOAc/hexane). After complete consumption of the epoxide/thiirane, the volume of the reaction mixture was concentrated under reduced pressure and the residue was triturated with diethyl ether. The catalyst thus separated was filtered and dried. The filtrate was concentrated to give the crude product, which was purified by gradient column chromatography using 60−120 mesh silica and EtOAc/hexane as the eluent. The recovered catalyst was reusable without purification.

Physical Measurements. The conductivity measurements were done in organic solvents or water using the digital conductivity bridge from Popular Traders, India (model number: PT-825). The elemental analysis data were obtained with an Elementar Analysensysteme GmbH Vario EL-III instrument. The NMR measurements were done using an Avance Bruker 300 MHz instrument. The infrared spectra (either as KBr pellets or as a mull in mineral oil) were recorded using a Perkin-Elmer FTIR-2000 spectrometer. The absorption spectra were recorded using a Perkin-Elmer *Lambda-25* spectrophotometer. Mass spectra were recorded with the LC-TOF (KC-455) spectrometer of Waters. GCMS studies were done with the Shimadzu-2010

(35) (a) Sharma, S. K.; Upreti, S.; Gupta, R. *Eur. J. Inorg. Chem.* **2007**, 3247. (b) Singh, J.; Hundal, G.; Gupta, R. *Eur. J. Inorg. Chem.* **2008**, 2052. (c) Singh, J.; Hundal, G.; Gupta, R. *Polyhedron* **2007**, *26*, 3893.

instrument containing an Rtx-5MS-30 Mt column of 0.25 mm internal diameter.

Crystallography. Single crystals suitable for X-ray diffraction studies were grown by the vapor diffusion of diethyl ether to a DMF (for **5**) or DMSO (for **6**) solution of the compound. X-ray diffraction studies of a suitably sized crystal, inserted in a quartz capillary filled with the mother liquor, were carried out on a BRUKER AXS SMART-APEX diffractometer equipped with a CCD area detector (Mo Kα = 0.71073 Å, monochromator: graphite).[36] Frames were collected at 298 K by ω,ϕ and 2θ-rotation at 10 s per frame with SMART.[36] The measured intensities were reduced to F^2 and corrected for absorption with SADABS.[37] Structure solution, refinement, and data output were carried out with the SHELXTL program using direct methods.[38] Non-hydrogen atoms were refined anisotropically. The hydrogen atoms were placed in geometrically calculated positions by using a riding model. Disordered O atoms for the water molecules in **5** were located in difference Fourier maps and refined anisotropically using the free variable command, and the occupancies were fixed in the final refinement cycles. Noncovalent interactions in the crystal lattice were calculated with SHELXTL and Diamond.[38,39] Further details of the X-ray structural analyses for **5** and **6** are provided in Table 1.

Acknowledgment. R.G. is thankful to the Department of Science and Technology (DST), New Delhi, for the generous financial support. A.A. thanks UGC for the JRF fellowship. The authors also thank the crystallographic facility at the Department of Chemistry and Institute for Materials Research, State University of New York at Binghamton through NSF grant DMR - 0705657.

Supporting Information Available: Figures for absorption spectra (S1), ^{1}H and ^{13}C NMR spectra (S2 and S3), and a CIF file. This material is available free of charge via the Internet at http://pubs.acs.org.

(36) *SMART*, version 5.0 618; Bruker Analytical X-ray Systems: Madison, WI, **2000**.

(37) *SAINT-NT*, version 6.04; Bruker Analytical X-ray Systems: Madison, WI, **2001**.

(38) *SHELXTL-NT*, version 6.10; Bruker Analytical X-ray Systems: Madison, WI, **2000**.

(39) *DIAMOND*, version 2.1c; B. Klaus University of Bonn: Bonn, Germany, **1999**.